JOURNAL OF GEOPHYSICAL RESEARCH, VOL. 87, NO. C3, PAGES 1961–1967, MARCH 20, 1982

A Relationship Between Wind Stress and Wave Slope

WILLIAM J. PLANT

U.S. Naval Research Laboratory, Washington, D. C. 20375

Recently published data taken in wind-wave tanks and on the ocean are shown to yield a growth rate, β, describing the transfer of energy and momentum directly from wind to surface waves, that is well described by the relation $\beta = [(0.04 \pm 0.02)u_*^2\omega \cos\theta]/c^2$ over a wide range of frequencies. Here u_* is air friction velocity, ω is radian wave frequency, c is phase speed, and θ is the angle between wind and waves. Using this form and the requirement that the momentum flux from wind to waves not exceed the wind stress, we show that the total mean-square, upwind/downwind wave slope between the frequencies $g/2\pi U_{10}$ and 20 Hz must be less than $\rho_a/[\rho_\omega(0.04 \pm 0.02)]$, where ρ_a and ρ_ω are air and water densities, g is gravitational acceleration, and U_{10} is wind speed at 10 m. Measurements of mean-square slope both in wavetanks and on the ocean seem to show agreement with this limitation as long as the air-water interface is well defined. One implication of such a slope limitation is that mean slope spectral densities are limited to values which decrease as the peak frequency of a wind wave spectrum decreases. This may provide an explanation for the observation that mean-square, dominant wave slopes are typically smaller on the ocean than in wavetanks.

1. INTRODUCTION

A large amount of data on wind-generated waves has been collected recently which, when synthesized, yields a rather coherent picture of wind wave growth and equilibrium. The JONSWAP experiments of *Hasselmann et al.* [1973] have shown the importance of third-order, nonlinear interactions in the development of a spectrum of wind-generated waves. Wavetank experiments by *Wu et al.* [1977, 1979] and by *Plant* [1980] have further established the role of these nonlinear interactions. Thus in many cases, growth rates of waves whose frequencies are lower than the dominant wave frequency are primarily determined by a transfer of energy and momentum from the dominant wave region rather than by transfer directly from the wind. This view is supported by recent electromagnetic scattering experiments of *Stewart and Teague* [1980] who measured spatial growth rates of 7 s waves in the Gulf of Mexico. They obtained growth rates in agreement with JONSWAP measurements but independent of the ratio of wind speed to wave speed and larger than expected from direct wind input. Comprehensive measurements of this direct, wind-induced input have recently been made in the Bight of Abaco [*Snyder et al.*, 1981] and confirm that wind-induced growth rates are much smaller than those measured by Stewart and Teague. Further support for the view that wave growth is often dominated by nonlinear interactions came from measurements of initial temporal growth of waves in a wind-wave tank carried out by *Plant and Wright* [1977]. They found that growth rates of waves longer than 10 cm were larger than those necessary if the waves were to support all the wind stress. They proposed that these waves grew primarily by nonlinear energy transfer from shorter waves even in their initial stages.

Growth rates due to the direct input of energy and momentum from wind to waves may be determined by measuring the initial growth of waves shorter than 10 cm or by measuring the wave-induced pressure field above waves of any length. Measurements of the former type have been made by *Larson and Wright* [1975] and by *Kawai* [1979] in wind-wave tanks. Wave-induced pressure measurements have been carried out in wavetanks by *Shemdin and Hsu* [1967] and by *Wu et al.* [1977, 1979] and on the ocean by *Dobson* [1971], *Elliott* [1972], *Snyder* [1974] and *Snyder et al.* [1981]. Initial growth measurements indicate that a frequency exists (about 20 Hz) at which the wind-induced growth rate maximizes; ocean measurements show that this growth rate falls rapidly as wave speed approaches wind speed. In the frequency range between these two extremes, however, a single, well-defined equation for the growth rate, β, due to direct energy and momentum transfer from wind to waves may be inferred from the data.

In section 2 of this paper we plot growth rates from several of the above experiments and show that they are consistent with the relation

$$\beta = \frac{(0.04 \pm 0.02)u_*^2\omega \cos\theta}{c^2} \tag{1}$$

for the wind-induced growth rate over the frequency range $g/2\pi U_{10}$ to 20 Hz. Here g is gravitational acceleration, U_{10} is wind speed at 10 m, u_* is air friction velocity, ω ($= 2\pi f$) is radian wave frequency, c is phase speed, and θ is the angle between wind and wave directions. This form has been previously noted in studies of short gravity waves [*Valenzuela and Wright*, 1976; *Plant and Wright*, 1977]; its similarity to those obtained in a number of theoretical studies is also discussed in section 2. In section 3, we use this form for the growth rate, along with the observation that it applies in the equilibrium state as well as the initial-growth state, to deduce a form for the momentum flux from wind to waves. Invoking the requirement that this flux always be less than the wind stress, we then deduce a limit on the total mean-square, upwind/downwind wave slope that may be contained in the frequency range from $g/2\pi U_{10}$ to 20 Hz. Section 4 contains a summary of slopes of wind-generated waves which have been measured in wavetanks and on the ocean. These are shown generally to conform to the expected limitation. Finally, in section 5, we discuss the implications of this relationship between wind stress and wave slope.

2. GROWTH RATES OF WIND WAVES

Initial temporal growth rates of wind-generated waves may be measured using electromagnetic (Bragg scattering)

Paper number 1C1633.

techniques in a very straightforward manner. In such measurements, the power, P, backscattered to the radar is proportional to the spectral intensity, $F(k, 0)$, of a wave of one particular wave number, k, propagating in the horizontal direction in which the antennas are pointing. Thus, if the wind speed is suddenly increased from zero, the time rate of change of P normalized by P is a direct measure of growth rate. If the antennas point in the wind direction, we have

$$\frac{1}{P}\frac{\partial P}{\partial t} = \frac{1}{F(k, 0)}\frac{\partial F(k, 0)}{\partial t} \equiv \beta'(k, 0) \tag{2}$$

where we used β' to indicate a growth rate which may be caused either by nonlinear effects or directly by the wind. Since a dispersion relation exists between frequency f and wave number k, during these early growth stages, $\beta'(f, 0)$ may be obtained from $\beta'(k, 0)$. Initial spatial growth rates such as those of *Stewart and Teague* [1980] are measured in a very similar manner using these techniques except that $\partial F/\partial x$ is measured at a constant wind speed and $\partial F/\partial t$ is determined by multiplying by group speed.

The determination of growth rates from measurements of wave-induced pressure fluctuations is somewhat more involved. The rate of work done on a progressive surface wave by atmospheric pressure is [*Phillips*, 1977]

$$\frac{\partial E(f, \theta)}{\partial t} = -\operatorname{Re}(\overline{p^* w})/2 \tag{3}$$

where E is the wave energy, p is the wave-induced air pressure, and w is the vertical component of surface velocity. (The asterisk indicates the complex conjugate, while 'Re' means 'real part of.') Let

$$p = \rho_a \omega c \gamma \eta \tag{4}$$

where ρ_a is air density, η is the amplitude of the wave of frequency f propagating at the angle θ to the wind and γ is a complex dimensionless function of f, θ and wind speed which is to be determined. Using (4) along with the (first order) relations

$$E(f, \theta) = \rho_w c \omega F(f, \theta) \tag{5}$$

$$w = -i\omega\eta \tag{6}$$

and

$$\tfrac{1}{2}\overline{\eta^* \eta} \equiv F(f, \theta) \tag{7}$$

(3) becomes

$$\frac{\partial F(f, \theta)}{\partial t} = \left(\frac{\rho_a}{\rho_w}\right) \omega\, [\operatorname{Im} \gamma(f, \theta)] F(f, \theta) \tag{8}$$

where 'Im γ' indicates the imaginary part of γ and $F(f, \theta)$ is wave height spectral density. Thus we identify

$$\beta(f, \theta) = \left(\frac{\rho_a}{\rho_w}\right) \omega \operatorname{Im} \gamma(f, \theta) \tag{9}$$

In this case, only direct effects of the wind are included in the growth rate so we use β instead of β'. With a single pressure transducer, the function usually measured is the cross-spectrum of pressure and waveheight, $G_{p\eta}(f)$. We have

$$G_{p\eta}(f) = \rho_a \int \omega c \gamma^*(f, \theta) F(f, \theta)\, d\theta \tag{10}$$

Making the normal assumptions for angular dependence,

$$\beta(f, \theta) = \beta(f) \cos \theta$$

$$F(f, \theta) = F(f)\left[\frac{2}{\pi}\cos^2 \theta\right] \qquad |\theta| < \frac{\pi}{2} \tag{11}$$

and using (9), we find

$$\beta(f) \equiv \beta(f, 0) = \left(\frac{3\pi}{8}\right)\frac{\operatorname{Im} G_{p\eta}^*(f)}{\rho_w c F(f)} \tag{12}$$

Since the pressure is necessarily measured at some height above the water surface, measurements of $G_{p\eta}(f)$ are corrected by extrapolating to the surface, usually using potential theory.

In Figure 1, we plot growth rates determined in a variety of electromagnetic-scattering and pressure-sensing experiments for $u_* = 0.45$ m/s. Where u_* was not given in the original paper, we have used the plots of u_* versus various measured wind speeds given by *Amorocho and DeVries* [1980]. We have found these curves to be a good representation of u_* versus wind speed in all cases where such a relationship was measured. In particular, they agree with values obtained by *Snyder et al.* [1981] and by *Plant and Wright* [1977]. Thus we will continue this practice throughout the present paper. The shaded area in Figure 1 indicates growth rates deduced from the work of *Snyder et al.* [1981] using their 'best guess' for Im $\gamma(f, \theta)$. This was given by

$$\operatorname{Im} \gamma \sim (0.2 \text{ to } 0.3)\left(\frac{U_5 \cos \theta}{c} - 1\right) \tag{13}$$

where U_5 is the wind speed at 5 m. The solid and dashed lines in this figure correspond to $\beta(f)$ as given by (1); effects of wind drift are included in the phase speed [*Plant and Wright*, 1979, 1980] so that they agree with measured phase speeds. Conversion of $\beta(k, 0)$ given by *Larson and Wright* [1975], *Plant and Wright* [1977], and *Stewart and Teague* [1980] to $\beta(f, 0)$ was accomplished using the steady state dispersion relation given by *Plant and Wright* [1980].

Also shown in Figure 1 are theoretical values of growth rates inferred from Figure 17 of *Kawai* [1979] for the case when the thickness of the viscous sublayer is eight times the ratio of the kinematic viscosity of air to its friction velocity. Kawai referred to waves of the wave number corresponding to the highest growth rate as 'initial wavelets' since they are the first to appear in a spectrum. Only growth rates of these initial wavelets were measured in his experiments but these agreed well with his maximum theoretical growth rates. Those shown in Figure 1 correspond to a steady state air friction velocity of 43 cm/s.

Maximum deviation from (1) of the growth rates shown in Figure 1 occurs for three cases. These are as follows:

1. Measurements of initial spatial or temporal growth rates of waves longer than 10 cm. As pointed out in the introduction, it is rather well established that the growth of such waves is primarily due to nonlinear interactions. Thus these measurements should not be considered when the

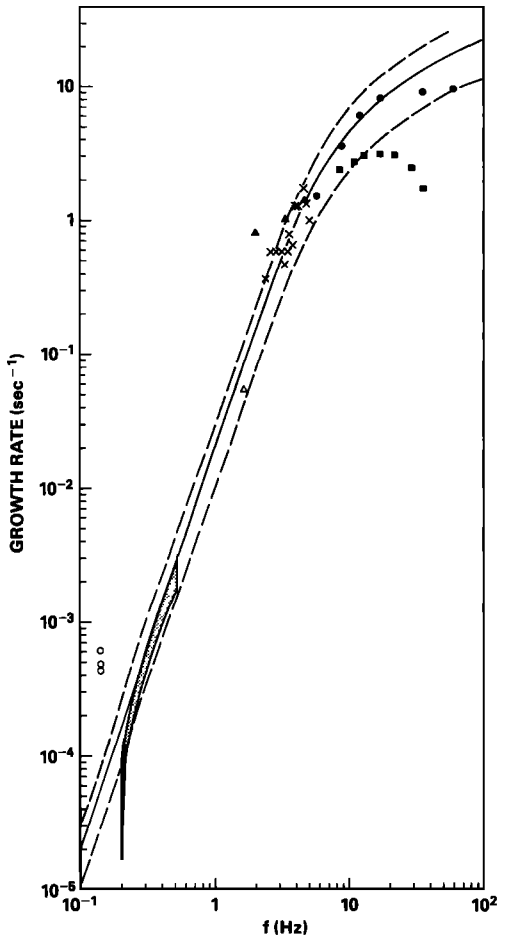

Fig. 1. Growth rate versus wave frequency for $u_* = 0.45$ m/s. Solid and dashed lines represent (1). Solid squares are theoretical values inferred from *Kawai* [1979]; the largest of these values agrees with his measured 'initial wavelet' growth rates. Shaded area indicates growth rates inferred from the empirical relation for quadrature pressure given by *Snyder et al.* [1981]. Experimental values from wavetanks: open triangles, *Shemdin and Hsu* [1967]; solid circles, *Larson and Wright* [1975]; solid triangles, *Plant and Wright* [1977]; crosses, *Wu et al.* [1977, 1979]; open circles, *Stewart and Teague* [1980].

direct transfer of energy and momentum from wind to waves is being determined.

2. Growth rates of waves traveling at or near the wind speed. Since momentum transfer from wind to wave is not expected to occur for waves traveling faster than the wind, the form of (1), which describes only this direct transfer, cannot hold at these frequencies. Note that the large growth rates measured by Stewart and Teague for waves which were traveling faster than the wind reaffirm that these waves grow primarily due to third-order, nonlinear interactions.

3. Growth rates of waves whose frequencies are near 20 Hz. Both the study of Larson and Wright and that of Kawai showed that a definite maximum occurs in the growth rate at high frequencies. Both studies clearly demonstrate that growth rates of waves whose frequencies are above about 20 Hz fall below those predicted by (1) for all wind speeds up to $u_* = 1.20$ m/s.

Figure 2 shows $\beta(f, 0)/f$ versus u_*/c for a variety of measurements of the wind-induced growth rate for u_* up to 1.20 m/s. Values obtained from waves whose frequencies were near or above those of initial wavelets (generally about 20 Hz) were excluded from this plot. Once again, solid and dashed lines indicate (1). The dashed lines, in fact, correspond to 95% confidence intervals for the part of this data set which is above $u_*/c = 0.07$. These data fit the form of (1) over almost two orders of magnitude variation in u_*/c and more than three orders of magnitude variation in growth rate. Thus in the frequency range between the frequency at which wind speed equals wave phase speed and about 20 Hz, (1) well describes the growth of surface waves induced directly by the wind.

The form of (1) is not without theoretical justification for the case when wind and waves are parallel. For this case, *Miles* [1959] obtained the form

$$\beta = \frac{\rho_a \xi u_*^2 \omega}{\kappa^2 \rho_w c^2} - 4\nu\omega^2/c^2 \tag{14}$$

where κ is von Kármán's universal turbulence constant and ξ is a function of u_*/c which falls from about 3.3 for $u_*/c > 0.1$ to zero as u_*/c approaches 0.05. Substituting $\xi = 3.3$ into (14) yields

$$\beta = \frac{0.025 u_*^2 \omega}{c^2} - 4\nu\omega^2/c^2 \tag{15}$$

The first term agrees well with (1) while the second term, which accounts for viscous damping, causes β to maximize at high frequencies. If measured phase speeds are used in (15), the maximum predicted growth rate generally occurs at much higher frequencies than observed experimentally.

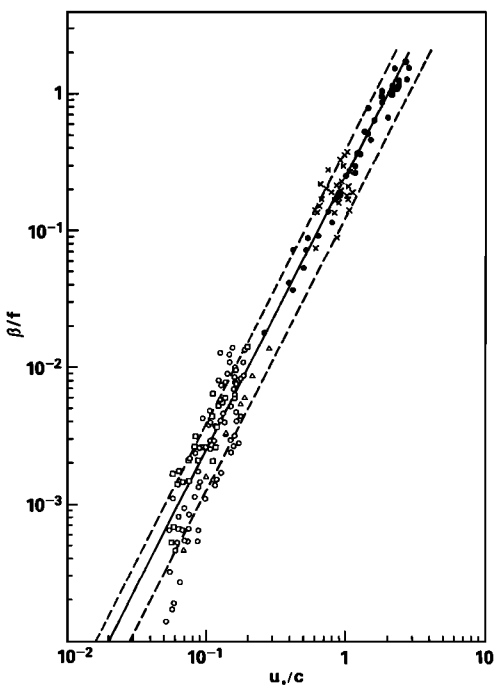

Fig. 2. Wind-induced growth rate, $\beta(f, 0)$, normalized by wave frequency versus friction velocity per unit phase velocity. Solid and dashed lines represent (1). triangles, *Shemdin and Hsu* [1967]; solid circles, *Larson and Wright* [1975]; crosses, *Wu et al.* [1977, 1979]; open circles, *Snyder et al.* [1981], fixed sensors; squares, *Snyder et al.* [1981], wave-following sensor.

More exact numerical calculations of β, which include shear flow in the water, yield frequencies corresponding to maximum growth rates which are in better agreement with experiment [*Valenzuela*, 1976; *Kawai*, 1979].

Townsend [1972] in his study of wave-induced oscillations of pressure and turbulent Reynolds stresses above an air-water interface deduced a growth rate given by

$$\beta = 15\left(\frac{\rho_a}{\rho_w}\right)\left(\frac{u_*}{c}\right)^2 \omega \tag{16}$$

which is lower than, but close to, the form given in (1). Finally, *Stewart* [1974] outlines a three-dimensional theory (he calls it 'crude') from which growth rates given by

$$\beta = 0.04\left(\frac{\rho_a}{\rho_w}\right)\omega\left[\frac{U^2}{c^2} - \frac{U}{c}\right] \tag{17}$$

may be inferred. Here U is wind speed; if we take it to be $25u^*$ and much larger than the phase speed, we have

$$\beta = 0.043\left(\frac{u_*}{c}\right)^2 \omega \tag{18}$$

in excellent agreement with (1).

3. A Limitation on Wind-Wave Slopes

The stress (momentum flux) applied to a system of waves by the wind may be written

$$\tau_w = \int_{-\pi}^{\pi}\int_0^{\infty}\int_0^{\infty} \beta(f, k, \theta)\,\mathbf{M}(f, k, \theta)\,k\,dk\,df\,d\theta \tag{19}$$

where β is the rate of growth induced by the wind and $\mathbf{M}$ is the momentum of the wave of wavenumber k and frequency f which is traveling in the direction θ with respect to the wind. For irrotational waves,

$$\mathbf{M}(f, k, \theta) = \frac{E(f, k, \theta)}{\mathbf{c}} = \omega\rho_w F(f, k, \theta)\hat{a}_m \tag{20}$$

where $\hat{a}_m$ is a unit vector in the direction of $\mathbf{M}$. Rotational effects may be included in this equation by taking ω to be the wave frequency in the presence of shear flow in the water. Using (1) for the wind-induced growth rate and (20) for $\mathbf{M}$, (19) becomes

$$\tau_w = (0.04 \pm 0.02)\rho_w u_*^2 \int_{-\pi}^{\pi}\int_{f_w}^{f_i}\int_0^{\infty} k^3 \cos\theta \cdot F(f, k, \theta)\hat{a}_m\,dk\,df\,d\theta \tag{21}$$

where the form of β has been truncated at $f_w = g/2\pi U_{10}$ and $f_i = 20$ Hz. The component of this stress in the direction of the wind is

$$\tau_w = (0.04 \pm 0.02)\rho_w u_*^2 \int_{f_w}^{f_i}\left[\int_{-\pi}^{\pi}\int_0^{\infty} k^3 \cos^2\theta \cdot F(f, k, \theta)\,dk\,d\theta\right] df \tag{22}$$

But the frequency spectrum of upwind/downwind slopes is

$$S_u(f) = \int_{-\pi}^{\pi}\int_0^{\infty} k^3 \cos^2\theta\, F(f, k, \theta)\,dk\,d\theta \tag{23}$$

so

$$\tau_w = (0.04 \pm 0.02)\rho_w u_*^2 \int_{f_w}^{f_i} S_u(f)\,df \tag{24}$$

Since this stress must be less than the wind stress, $\rho_a u_*^2$, we have the following limitation on upwind/downwind slope:

$$\int_{f_w}^{f_i} S_u(f)\,df \le \frac{\rho_a}{(0.04 \pm 0.02)\rho_w} = 0.04 \pm 0.02 \tag{25}$$

where ρ_a and ρ_w have been evaluated at 20°C.

An equivalent derivation of this relationship may be developed by assuming that the growth rate at a particular frequency may be obtained from (1) by replacing k^2 by a mean value of k^2:

$$\overline{k^2} = \frac{1}{F(f, \theta)}\int_0^{+\infty} k^3 F(f, k, \theta)\,dk \tag{26}$$

Then (25) follows immediately from the definition $S_u(f) = \int_{-\pi}^{\pi} \overline{k^2}\cos^2\theta\, F(f, \theta)\,d\theta$.

Truncation of the expression for β at f_w and f_i is obviously an approximation to the true behavior of the wind-induced growth rate. The low frequency roll-off exhibited by the data is quite sharp so that truncation at f_w should be a rather good approximation. The high-frequency roll-off of β, however, is more gradual and deserves closer examination. If (1) for β were multiplied by a factor $\Phi(f)$ and continued to high frequencies, then (25) would read

$$\int_{f_w}^{\infty} \Phi(f)S_u(f)df \le 0.04 \pm 0.02 \tag{27}$$

If we take $\Phi(f)$ to be of the form

$$\begin{aligned} \Phi(f) &= 1 \qquad f < 8 \text{ Hz} \\ \Phi(f) &= 8/f \qquad f \ge 8 \text{ Hz} \end{aligned} \tag{28}$$

then β rolls off at high frequencies in a manner similar to that calculated by Kawai. Using this form, it is easy to show that the left side of (27) differs from that of (25) by a maximum of 0.001 using realistic slope spectral values as discussed below. Since this difference is much less than the uncertainty on the right side, the precise form of the high-frequency roll-off of β is not crucial in evaluating (27). Thus truncation of β at 20 Hz, which yields (25), should be sufficiently accurate. Note that this cut-off frequency corresponds to mean wavelengths longer than 1.2 cm so that effects of capillarity over the frequency range of interest will be small.

4. Comparison With Experiment

Measurements of upwind/downwind slopes in wind-wave tanks have been reported by several authors, notably *Cox* [1958], *Wu* [1971], *Keller et al.* [1974], *Long and Huang* [1976], *Plant* [1980], and *Lleonart and Blackman* [1980]. The papers by Keller et al. and by Plant report only dominant wave slopes, i.e., spectral integrals up to 1.5 times the dominant wave frequency. However, during the course of the experiments leading to the latter paper, the author measured more than 50 upwind/downwind slope spectra for frequencies up to 20 Hz and above using Cox's optical method [*Plant*, 1980]. Figure 3 shows three of these measured spectra up to 20 Hz. Integration of these spectra up to 60 Hz gave mean-square upwind/downwind slopes which

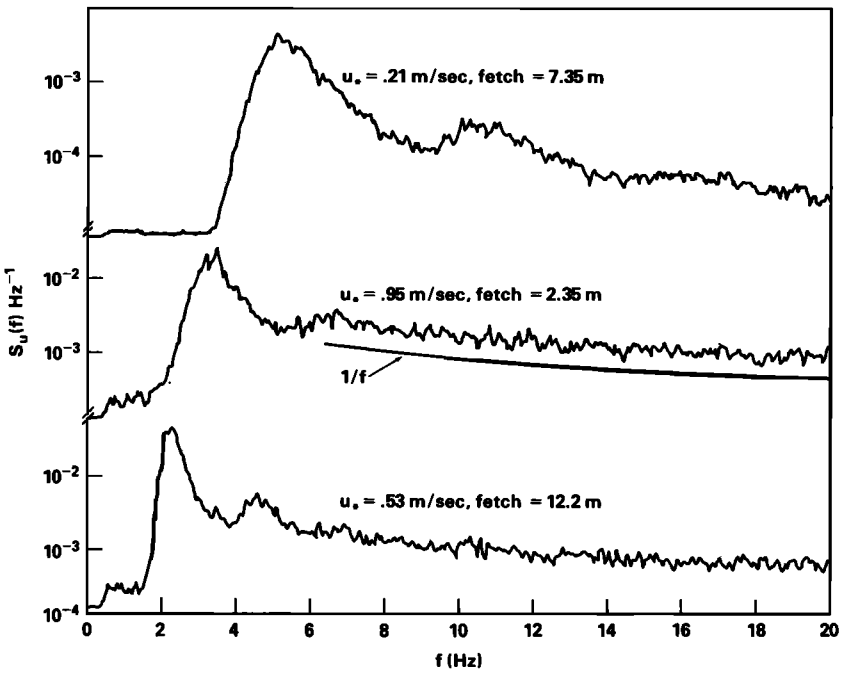

Fig. 3. Upwind/downwind slope spectra measured in a wind-wave tank for three different wind speed and fetch combinations.

were in good agreement with the results of both Cox and Wu. The mean-square upwind/downwind slopes between f_w and 20 Hz computed from these spectra are presented in Figure 4 as a function of the peak frequency f_p of the slope spectrum. Values derived from the work of other investigators are also shown in Figure 4 and will be discussed below.

The papers by *Cox* [1958], *Long and Huang* [1976], and *Lleonart and Blackman* [1980] all present upwind/downwind slope spectra which can be integrated from f_w to 20 Hz. Such integrals from the work of Lleonart and Blackman are plotted in Figure 4. Integrals of spectra presented in the other two papers, however, yield mean-square values which are higher than those presented in the papers without spectral analysis. In order to correct this, the presented upwind/downwind spectra were normalized to yield integrals equal to 0.75 times the total mean-square slope as would be proper for a $\cos^2 \theta$ angular distribution. These spectra were then integrated between f_w and 20 Hz to obtain the values presented in Figure 4.

The dashed line in this figure corresponds to the maximum value given by the right side of (25). The vast majority of the data are seen to lie below this line as expected. The highest two wavetank data points obtained by the author are presented for completeness. There is some evidence that data taken at high winds such as these ($u_* = 1.20$ m/s) may not be accurate due to the presence of spray which can reflect extraneous light into the telescope. Indeed, at such high winds, the concept of a connected wavy surface with well-defined slopes begins to break down and results based on this picture are necessarily suspect.

Measurements of slope spectra on the ocean are more difficult to obtain. The classic work in this area is that of *Cox and Munk* [1954] who inferred sea surface slopes from sun glitter patterns. *Wentz* [1976] has shown that Cox and Munk's data can only set a lower limit on mean square slopes. However, since slopes which cannot be measured by Cox and Munk's method are those which are 'large and infrequent' according to Wentz, their data should provide a reasonably good estimate of wind-wave slopes. Maximum mean-square upwind/downwind slopes obtained by Cox and Munk were about 0.048 at $u^* = 0.7$ m/s. When an oil slick was present on the surface a maximum value of about 0.013 was obtained at $u^* = 0.4$ m/s. Spectra taken at wind speeds of 5 and 10 m/s for both a clean and slick-covered surface are

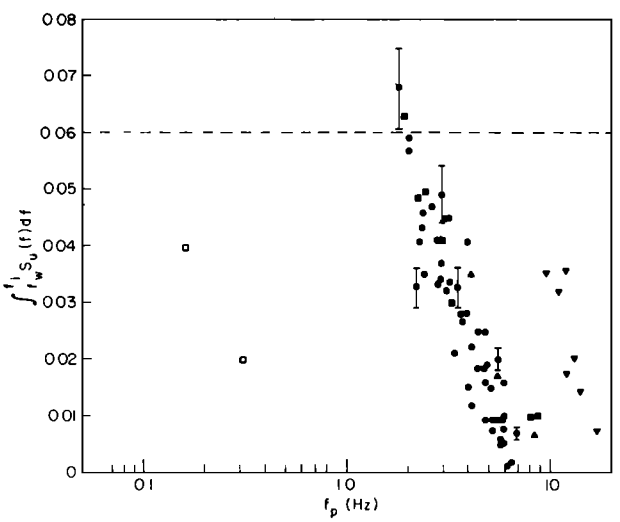

Fig. 4. Mean-squared, upwind/downwind wave slope between f_w and 20 Hz versus peak frequency of the slope spectrum. The dashed line represents the maximum value given by (25). Closed circles were computed by integration of wavetank spectra obtained by the author. Other closed symbols were derived from wavetank measurements by other investigators as described in the text. up-pointing triangles, *Cox* [1958]; squares, *Long and Huang* [1976]; down-pointing triangles, *Lleonart and Blackman* [1980]. The two open squares are values inferred from field measurements of *Cox and Munk* [1954] as described in the text.

presented by Cox and Munk. These spectra indicate that the method was capable of measuring slopes of waves up to well above 100 Hz but that waves with frequencies above about 1 Hz were severely damped by the slick. Thus one would expect the integral of (25) to be between 0.013 and 0.048. If one integrates the two clean-surface spectra up to 20 Hz and multiplies by 3/4 to get upwind/downwind slopes, the points plotted in Figure 4 are obtained. These are somewhat above the total mean-squared, upwind/downwind slopes given by Cox and Munk at the same windspeed but well below the 0.06 limit.

Recent measurements of high frequency slope spectra using a wave-following laser slope meter have been reported by *Lubard et al.* [1980]. Their results indicate that such spectra follow an f^{-1} law to a good approximation at a wind speed of 7.5 m/s. This observation agrees with a variety of wavetank measurements (Figure 3, *Cox* [1958], *Long and Huang* [1976], *Lleonart and Blackman* [1980]). If we assume it to hold for a variety of oceanic conditions, then we may approximate the upwind/downwind slope spectrum as follows:

$$\begin{aligned} S_u(f) &= 0.75k^2F(f) \qquad 0 < f < 1.5f_m \\ S_u(f) &= \alpha'/f \qquad\qquad 1.5f_m < f \end{aligned} \tag{29}$$

where $F(f)$ is any standard spectrum applicable near the dominant wave frequency and a $\cos^2\theta$ angular dependence has been used. Substituting this into (25), we get

$$0.75\int_{f_w}^{1.5f_m} k^2F(f)\,df + \alpha'\int_{1.5f_m}^{f_i}\frac{df}{f} \le 0.04 \pm 0.02 \tag{30}$$

Since a dispersion relation exists in the neighborhood of the dominant wave frequency, it is straightforward to evaluate $S_u(f)$ below $1.5f_m$ using, say, a JONSWAP or Pierson-Moskowitz spectrum [*Hasselmann et al.*, 1973; *Pierson and Moskowitz*, 1964]. Doing so, we find that the first integral in (30) is generally less than 0.01 so that α' must generally conform to the following limit if (25) is valid:

$$\alpha' \le \frac{0.05}{\ln(13.3/f_m)} \tag{31}$$

Here we have let $f_i = 20$ Hz. For typical oceanic dominant wave frequencies, this requires α' to be less than about 0.012, the value which makes $S_u(f)$ in (29) continuous for JONSWAP or P-M spectra. Spectra presented by *Lubard et al.* [1980] indicate that α' is about 0.001 at 7.5 m/s. It is plausible to assume that these high-frequency spectral densities increase with wind speed in the same manner as the radar backscatter cross sections measured by *Jones et al.* [1977]. If this is the case, then high-frequency slope spectral densities are still below the limit imposed by (31) at a windspeed of 23.6 m/s, the highest at which Jones et al. made measurements. As in the wavetank, however, the concept of high-frequency waves with measurable slopes must break down at sufficiently high wind speeds.

5. DISCUSSION AND IMPLICATIONS

The primary results of this paper are contained in (1) and (25). These results apply to the growth and equilibrium of deep-water surface waves under the action of a steady wind in the absence of large swell propagating in random directions. The wind speed is assumed to be low enough to allow the air-water interface to be well defined. It has been shown that both theory and experiment support the form of (1) to describe the frequency, wavenumber, and wind speed dependence of wind-induced growth rates. The angular dependence of β given by (1) agrees with that found in the Bight of Abaco experiment [*Snyder et al.*, 1981]. Small deviations from this angular dependence should have little effect on present results. The validity of (25) depends upon an extension of results valid for irrotational waves to rotational waves by including shear flow effects in the dispersion relation, and on the truncation of the form of β which has already been discussed. Since the integral in (25) does not reach much beyond the frequency at which capillary effects enter, rotational effects should not dominate the calculation. Available data seem to support the slope limitation imposed by (25).

In fact, Figure 4 shows that data for $f_p < 3$ Hz generally fall within the limits established by the equality in (25). This is consistent with the hypothesis of *Plant and Wright* [1977] that surface waves support essentially all of the wind stress when the dominant wavelength is longer than 10 cm. If this is indeed the case, then the typical observation that mean-square dominant wave slopes are smaller on the ocean than in wavetanks is plausibly explained. If $f_m > f_w$, the range of frequencies available to produce a mean-squared, upwind/downwind slope of 0.04 ± 0.02 as given by (25) is that from just below f_m up to 20 Hz. On the ocean this range is wider than in wavetanks so the mean slope spectral density is expected to be smaller on the ocean. The distribution of the reduction of slope across the spectrum depends on nonlinear interactions and dissipation, making its form difficult to predict. However, the observation that waveheight spectra are more peaked in wavetanks than on the ocean [*Plant*, 1980] indicates that the ratio of slope spectral density near the dominant wave frequency to that at higher frequencies is smaller on the ocean than in wavetanks. The reduction in mean slope spectral density thus implies a reduction of mean-square dominant wave slope. Smaller oceanic dominant wave slopes imply that spectral manifestations of second harmonics of Stokes waves should be smaller on the ocean than in wavetanks. Indeed they are generally not observed in ocean wave spectra although they are prominent in wavetank spectra (Figure 3, *Pierson and Moskowitz* [1964], *Mitsuyasu* [1968], *Hasselmann et al.* [1973]).

REFERENCES

Amorocho, J., and J. J. DeVries, A new evaluation of the wind stress coefficient over water surfaces, *J. Geophys. Res.*, *85*, 433–442, 1980.

Cox, C. S., Measurements of slopes of high-frequency wind waves, *J. Mar. Res.*, *16*, 199–225, 1958.

Cox, C. S., and W. Munk, Statistics of the sea surface derived from sun glitter, *J. Mar. Res.*, *13*, 198–227, 1954.

Dobson, F. W., Measurements of atmospheric pressure on wind-generated sea waves, *J. Fluid Mech.*, *48*, 91–127, 1971.

Elliott, J. A., Microscale pressure fluctuations near waves being generated by the wind, *J. Fluid Mech.*, *54*, 427–448, 1972.

Hasselmann, K., et al., Measurements of wind-wave growth and swell decay during the Joint North Sea Wave Project (JONSWAP), *Dtsch. Hydrogr. Z. Suppl. A*, *12*, 1–95, 1973.

Jones, W. L., L. C. Schroeder, and J. L. Mitchell, Aircraft measurements of the microwave scattering signature of the ocean, *IEEE J. Ocean Eng.*, *OE-2*, 52–67, 1977.

Kawai, S., Generation of initial wavelets by instability of a coupled shear flow and their evolution to wind waves, *J. Fluid Mech.*, *93*, 661–703, 1979.

Keller, W. C., T. R. Larson, and J. W. Wright, Mean speeds of wind waves at short fetch, *Radio Sci., 9,* 1091–1100, 1974.

Larson, T. R., and J. W. Wright, Wind-generated gravity-capillary waves: Laboratory measurements of temporal growth rates using microwave backscatter, *J. Fluid Mech., 70,* 417–436, 1975.

Lleonart, G. T., and D. R. Blackman, The spectral characteristics of wind-generated capillary waves, *J. Fluid Mech., 97,* 455–479, 1980.

Long, S. R., and N. E. Huang, On the variation and growth of wave-slope spectra in the capillary range with increasing wind, *J. Fluid Mech., 77,* 209–228, 1976.

Lubard, S. C., J. E. Krimmel, L. R. Thebaud, D. D. Evans, and O. H. Shemdin, Optical image and laser slope meter intercomparisons of high-frequency waves, *J. Geophys. Res., 85,* 4996–5002, 1980.

Miles, J. W., On the generation of surface waves by shear flows, 2, *J. Fluid Mech., 6,* 568–582, 1959.

Mitsuyasu, H., On the growth of the spectrum of wind-generated waves, 1, *Rep. Res. Inst. Appl. Mech. Kyusha Univ., 16,* 459–482, 1968.

Phillips, O. M., *The Dynamics of the Upper Ocean,* p. 49, Cambridge University Press, New York, 1977.

Pierson, W. J., Jr., and L. Moskowitz, A proposed spectral form for fully developed wind seas based on the similarity theory of S. A. Kitaigordskii, *J. Geophys. Res., 69,* 5181–5189, 1964.

Plant, W. J., On the steady-state energy balance of short gravity wave systems, *J. Phys. Oceanogr., 10,* 1340–1352, 1980.

Plant, W. J., and J. W. Wright, Growth and equilibrium of short gravity waves in a wind-wave tank, *J. Fluid Mech., 82,* 767–793, 1977.

Plant, W. J., and J. W. Wright, Spectral decomposition of short gravity wave systems, *J. Phys. Oceanogr., 9,* 621–624, 1979.

Plant, W. J., and J. W. Wright, Phase speeds of upwind and downwind traveling short gravity waves, *J. Geophys. Res., 85,* 3304–3310, 1980.

Shemdin, O. H., and E. Y. Hsu, Direct measurement of aerodynamic pressure above a simple progressive gravity wave, *J. Fluid Mech., 30,* 403–416, 1967.

Snyder, R. L., A field study of wave-induced pressure fluctuations above surface gravity waves, *J. Mar. Res., 32,* 497–531, 1974.

Snyder, R. L., F. W. Dobson, J. A. Elliott, and R. B. Long, Array measurements of atmospheric pressure fluctuations above surface gravity waves, *J. Fluid Mech., 102,* 1–59, 1981.

Stewart, R. H., and C. Teague, Dekameter radar observations of ocean wave growth and decay, *J. Phys. Oceanogr., 10,* 128–143, 1980.

Stewart, R. W., The air-sea momentum exchange, *Boundary Layer Meteorol., 6,* 151–167, 1974.

Townsend, A. A., Flow in a deep turbulent boundary layer over a surface distorted by water waves, *J. Fluid Mech., 55,* 719–735, 1972.

Valenzuela, G. R., The growth of gravity-capillary waves in a coupled shear flow, *J. Fluid Mech., 76,* 229–250, 1976.

Valenzuela, G. R., and J. W. Wright, The growth of waves by modulated wind stress, *J. Geophys. Res., 81,* 5795–5796, 1976.

Wentz, F. J., Cox and Munk's sea surface slope variance, *J. Geophys. Res., 81,* 1607–1608, 1976.

Wu, J., Slope and curvature distributions of wind-disturbed water surface, *J. Opt. Soc. Am., 61,* 852–858, 1971.

Wu, H. Y., E. Y. Hsu, and R. L. Street, The energy transfer due to air-input, non-linear wave-wave interaction and white cap dissipation associated with wind-generated waves, *Tech. Rep. 207,* pp. 1–158, Stanford Univ., Stanford, Calif., 1977.

Wu, H. Y., E. Y. Hsu, and R. L. Street, Experimental study of nonlinear wave-wave interaction and white-cap dissipation of wind-generated waves, *Dyn. Atmos. Oceans, 3,* 55–78, 1979.

(Received October 31, 1980;
revised October 1, 1981;
accepted October 19, 1981.)